

Synthesis of Ti-MWW by a dry-gel conversion method

Peng Wu^{a,*}, Takayuki Miyaji^b, Yueming Liu^a, Minyuan He^a, Takashi Tatsumi^{b,*}

^aShanghai Key Laboratory of Green Chemistry and Chemical Processes, Department of Chemistry,
East China Normal University, North Zhongshan Rd. 3663, Shanghai 200062, PR China

^bDivision of Materials Science and Chemical Engineering, Graduate School of Engineering, Yokohama National University,
79-5 Tokiwadai, Hodogaya-ku, Yokohama 240-8501, Japan

Available online 15 December 2004

Abstract

MWW type titanasilicate, Ti-MWW, has been synthesized by the dry-gel conversion (DGC) method, and its physicochemical properties and catalytic performance in the liquid-phase epoxidation of alkene have been compared with that of hydrothermally synthesized (HTS) Ti-MWW. The roles in the crystallization of silica source, alkali cation, cyclic amine as a structure-directing agent (SDA), and boric acid structure-supporting agent have been investigated. The crystallization of Ti-MWW did not occur for the dry gels free of boric acid, but was feasible at a Si/B molar ratio as high as 12 in marked contrast to the ratio of 0.75 required in the hydrothermal synthesis. The sodium as a mineralization agent was not necessary and on the contrary inhibited the crystallization particularly at a high content. The seeding technique using deboronated MWW effectively accelerated the crystallization speed and reduced the amount of boric acid required. As-synthesized Ti-MWW-DGC lamellar precursors contained both tetrahedral and octahedral species but the latter was selectively removed by acid treatment. Ti-MWW-DGC catalysts showed lower intrinsic activity than Ti-MWW-HTS in the epoxidation of hex-1-ene with hydrogen peroxide probably because the crystal size of the former was 10–20 times as large as that of the latter and then imposed significant diffusion problems for both the substrates and the products.

© 2004 Published by Elsevier B.V.

Keywords: Ti-MWW; Dry-gel conversion; Structure-supporting agent; Seeding method; Liquid-phase epoxidation

1. Introduction

Titanosilicates with isolated tetrahedral Ti species in the zeolite framework are highly efficient for the selective oxidation of a wide variety of organic substrates such as alkenes, alkanes, alcohols, aromatics, and ketones, etc. using environmentally friendly oxidant of hydrogen peroxide [1,2]. In order to meet the needs of various reactions and take advantage of various zeolitic crystalline structures, a variety of titanosilicates such as TS-1 [3], TS-2 [4], Ti-Beta [5], Ti-MOR [6], Ti-ITQ-7 [7], and Ti-MWW [8] have been prepared by the hydrothermal synthesis and the postsynthesis methods.

Among the above titanosilicates, Ti-MWW, with the structure analogue to MCM-22 aluminosilicate, especially demonstrates great potential for liquid-phase epoxidation catalyst showing extremely high specific activity for linear alkenes and unusual geometric selectivity for *cis/trans* alkenes in contrast to previous TS-1 and Ti-Beta [9–11]. These catalytic features of Ti-MWW essentially originate from its unique pore system consisting of side pockets, 10-membered ring (MR) channels containing supercages and independent sinusoidal 10 MR channels. Ti-MWW has been first prepared by the hydrothermal synthesis (HTS) method [8] and then by a novel structural conversion postsynthesis method [12]. In the hydrothermal synthesis, Ti-MWW can be crystallized only in the presence of boric acid, so-called structure-supporting agent, and a complete crystallization of gel needs a Si/B molar ratio of 0.75 corresponding to a large amount of boric acid in excess of that of silica [8]. Although both hydrothermally synthesized and postsynthesized Ti-MWW catalysts work well in the epoxidation reactions, it is

* Corresponding authors. Tel.: +86 21 6223 2292 (P. Wu)/+81 45 339 3943 (T. Tatsumi); fax: +86 21 5252 0411 (P. Wu)/+81 45 339 3941 (T. Tatsumi).

E-mail addresses: pwu@chem.ecnu.edu.cn
(P. Wu), ttatsumi@ynu.ac.jp (T. Tatsumi).

still worth searching for other synthesis processes which may develop more effective ones.

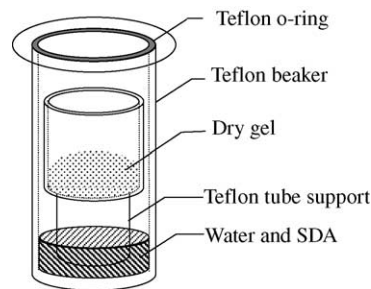
Besides the conventional HTS method, the dry-gel conversion (DGC) proves a useful preparing technique for several zeolite structures such as MFI [13], BEA [14], FER [15], MOR [16], and MTW [17]. The DGC method is theoretically applicable to any kind of structure-directing agent (SDA), whether it is volatile or not. The DGC crystallization using non-volatile SDAs is realized through the steam assisted crystallization (SAC) of the dry gels containing SDA, while the crystallization using volatile SDAs takes place through the vapor-phase transport (VPT) of SDA and steam over dry gels. The DGC method allows the transformation of dry gel to zeolite at high yield, the shortening of crystallization time, and the reduction of organic material consumption [13]. More importantly, the DGC method shows advantages not shared by the HTS method in the synthesis of BEA zeolite. Both BEA type aluminosilicate and titanosilicate synthesized by the DGC method have uniform crystals with much smaller particle size than those obtained by the HTS method. Ti-Beta-DGC thus prepared has been shown to be quite defect-less and hydrophobic, and then show higher intrinsic activity in the oxidation of cyclohexane than Ti-Beta-HTS [18,19]. The DGC method even allows the crystallization of Al-free Ti-Beta [20]; the HTS synthesis of Ti-Beta is only possible under the special conditions such as seeding method and the use of fluoride media.

In this study, we have applied the DGC method for the first time to the synthesis of Ti-MWW. The effects of silica source, SDA type, gel composition, and seed addition on the crystallization of Ti-MWW have been investigated. A particular effort has been made to reduce the amount of boric acid as a structure-supporting agent. In addition, Ti-MWW-DGC and Ti-MWW-HTS were comparatively characterized in terms of the physicochemical and catalytic properties.

2. Experimental

2.1. Synthesis of Ti-MWW

Two kinds of Ti-MWW have been prepared. The hydrothermally synthesized samples, designated as Ti-MWW-HTS, were prepared following the procedures described in detail elsewhere [8], while the DGC-synthesized samples, designated as Ti-MWW-DGC, were prepared by the vapor phase transport method. In a typical DGC synthesis run, tetrabutyl orthotitanate (TBOT, 97 wt.%, Kanto) was hydrolyzed in an aqueous solution containing hydrogen peroxide (31 wt.%, MGC) to avoid the formation of anatase. A clear Ti solution yellow in color was obtained after stirring the mixture at ambient temperature for 1 h. Boric acid (99.5 wt.%, Wako), serving as a crystallization-supporting agent, was dissolved in deionized water to which the mineralization agent of sodium hydroxide



Scheme 1. Special autoclave for the DGC synthesis.

(96 wt.%, Wako) was added if necessary. Above two solutions were mixed together before adding colloidal silica (ST-40, 40 wt.% SiO₂, Nissan) or fumed silica (Cab-o-sil M7D). The resultant homogeneous gel was stirred for 2 h, and then dried to evaporate water over an oil bath under continued stirring at 353 K, which resulted in a dry gel. The dry gel with a chemical composition of SiO₂: 0.017–0.033, TiO₂: 0–0.5, B₂O₃: 0–0.5; Na₂O was ground into fine powder. The powder (2 g) was transferred into a Teflon beaker placed in a special Teflon-lined autoclave (50 mL) where SDA of piperidine or hexametheleneimine (2 g) and water (1.5 g) were situated on the bottom (Scheme 1). The crystallization of the gel was performed by heating the autoclave statically at 443 K for 7–14 days. The solid product was washed with deionized water, dried at 353 K and calcined at 873 K for 10 h to remove organic matter. The as-synthesized Ti-MWW-DGC samples were refluxed with 2 M HNO₃ solution at a solid to liquid ratio of 1 g to 100 mL to extract the extraframework Ti together with a portion of framework B following the findings obtained with Ti-MWW-THS [8]. The acid-treated samples were further calcined in air at 873 K for 10 h.

2.2. Characterization methods

The samples were characterized with various techniques. X-ray diffraction patterns were collected on a MAC Science MX-Labo diffractometer using Cu K α radiation. UV–vis spectra were recorded on a JASCO V-550 spectrophotometer using BaSO₄ powder as a reference. N₂ adsorption measurements were carried out at 77 K on a Nihon BELSORP 28 A volumetric adsorption analyzer after the sample was outgassed at 373 K for 2 h. The amount of Ti and B was quantified by inductively coupled plasma emission spectrometry on a Shimadzu ICP-8000E spectrometer. The scanning electron microscopy (SEM) was performed on a Hitachi S-4200 instrument after suspending the sample in ethanol.

2.3. Catalytic reactions

The liquid-phase oxidation of hex-1-ene with hydrogen peroxide was carried out in a round-bottom flask (20 mL) fitted with a condenser and a magnetic stirrer. For a typical

run, a mixture of 0.05 g of catalyst, 10 mmol of hex-1-ene, 10 mmol of hydrogen peroxide (31 wt.% aqueous solution) and 10 mL of solvent (acetonitrile) was stirred vigorously at 333 K for 2 h. The reaction mixture was analyzed using a gas chromatograph (Shimadzu 14 B) equipped with a 50 m OV-1 capillary column, while the amount of hydrogen peroxide remaining in the reaction mixture was quantified by the titration with 0.1 M $\text{Ce}(\text{SO}_4)_2$ solution.

3. Results and discussion

3.1. Effect of various conditions on the crystallization Ti-MWW-DGC

The hydrothermal synthesis of MWW-type titanosilicate from the hydrogel of silicon and titanium only has been a great challenge still not successful so far. Nevertheless, we have developed a new method for the preparation of Ti-MWW; Ti is hydrothermally incorporated into the MWW structure using boric acid as a crystallization-supporting agent and hexametheleneimine (HMI) or piperidine (PI) as a SDA [8]. A big problem still lies in this method that the amount of boron necessary for crystallizing the MWW zeolite was even more than that of silicon, corresponding to a Si/B ratio of 0.75, in spite of the fact that the content of B in the final products was far lower than that in the initial hydrogel (Table 1, Nos. 1 and 2).

Thus, the effect of boron content on the crystallization of Ti-MWW-DGC has been investigated using the colloidal silica source and the SDA of HMI at a Si/Ti ratio of 60 (Table 1, Nos. 3–7). No additional sodium source was used in the preparation of the gel, while the Si/Na ratio of 37 corresponded to the impurity sodium in the colloidal silica. Fig. 1 shows the XRD patterns of the as-synthesized samples. While no crystalline phase was obtained from the

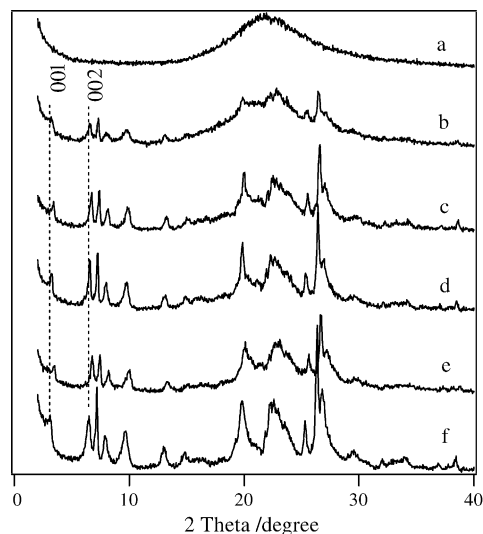


Fig. 1. XRD patterns of as-synthesized Ti-MWW-DGC samples synthesized from colloidal silica and HMI at Si/B ratio of ∞ (a), 12 (b), 5 (c), 3 (d), and 1 (e), and from fumed silica and HMI at Si/B ratio of 5 (f).

B-free dry gel, the MWW phase was formed at the Si/B ratio of 12 although being still low in crystallinity (Fig. 1a and b). On the other hand, the crystallization of the MWW phase progressed gradually with heating time at Si/B ratios of 5, 3 and 1, and was almost complete after 2 weeks (Fig. 1c–e). The XRD patterns of as-synthesized samples showed the 0 0 1 and 0 0 2 diffraction peaks corresponding to the typical MWW lamellar precursor. The layered structure consists of the MWW crystalline sheets between which the SDA molecules are probably inserted. As-synthesized Ti-MWW-DGC contained a relatively high amount of organic species corresponding to a SDA/Si molar ratio of 0.2 as evidenced by chemical analyses. After removal of the SDA species by calcination, the dehydroxylation took place between the sheets to cause the recrystallization throughout the crystals,

Table 1
Synthesis results of Ti-MWW by HTS and DGC methods^a

No.	Method	Silica source	Gel composition			SDA	Time (week)	Product			
			Si/Ti	Si/B	Si/Na			Phase ^b	Si/Ti	Si/B	Si/Na
1	HTS	Cab-o-sil	50	0.75	∞	HMI	1	MWW	53	12	∞
2	HTS	Cab-o-sil	50	0.75	∞	PI	1	MWW	51	11	∞
3	DGC	Colloidal	60	∞	37	HMI	2	Amor.			
4	DGC	Colloidal	60	12	37	HMI	2	Amor. + MWW			
5	DGC	Colloidal	60	5	37	HMI	2	MWW	61	17	114
6	DGC	Colloidal	60	3	37	HMI	2	MWW	58	13	135
7	DGC	Colloidal	60	1	37	HMI	2	MWW	54	13	325
8	DGC	Colloidal	60	5	37	PI	2	MWW	66	16	124
9	DGC	Colloidal	60	3	37	PI	2	MWW	84	14	–
10	DGC	Cab-o-sil	60	5	∞	HMI	2	MWW	84	14	∞
11	DGC	Cab-o-sil	60	5	∞	PI	2	MWW + Amor.			
12	DGC	Colloidal	60	5	5 ^c	HMI	2	Amor. + MWW			
13	DGC	Colloidal	60	5	3 ^c	HMI	2	Amor.			
14	DGC	Colloidal	60	5	1 ^c	HMI	2	Amor.			

^a Crystallization temperature 443 K.

^b Amor.: amorphous.

^c Na was supplied with NaOH.

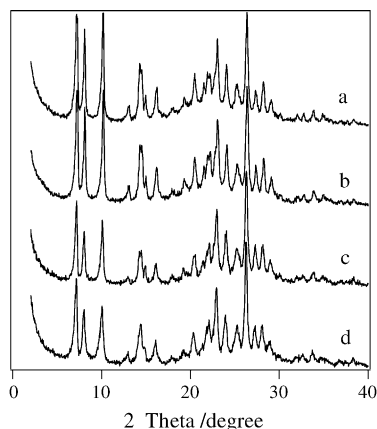


Fig. 2. XRD patterns of Ti-MWW-DGC samples after the calcination at 873 K for 10 h. The samples of (a–d) correspond to those of (c–f) shown in Fig. 1.

resulting in the formation of the three-dimensional MWW structure at the expense of the disappearance of the layered structure (Fig. 2). Like the previous hydrothermal synthesis, the DGC synthesis led to the incorporation nearly all titanium added in the gel into the solid product (Table 1). However, compared with Ti-MWW-HTS, the amount of B in Ti-MWW-DGC was generally smaller as a result of feasible crystallization at higher Si/B ratios.

The DGC method showed a great advantage; it is possible to synthesize Ti-MWW from the hydrogel containing only one fifth of the amount of boric acid required for the HTS method. Since boron is an element relatively difficult to occupy the tetrahedral sites in the zeolite framework because of its very small ionic size compared to silicon, a higher concentration of B in the hydrothermal gel would act as a kind of driving force favoring the introduction of soluble B species into the SiO₂ matrix during the nucleation and growth of crystallites. In the dry-gel conversion, the concentration of boron in the liquid phase in the hydrogel would be much higher than in the case of the HTS method because of the much smaller liquid/solid ratio in the DGC method. This would be the reason why Ti-MWW can be synthesized by the DGC method from the gels with relatively low boron amount, namely relatively high Si/B ratios.

The DGC-synthesis using PI as the SDA also resulted in the crystalline phase with the MWW structure (Table 1, Nos. 8 and 9). This is consistent with what has been observed in the hydrothermal synthesis, that is, HMI and PI are both suitable for the formation of Ti-MWW. In the DGC synthesis of either Al-containing or Al-free Ti-Beta, the function of mineralization agent of sodium species is indispensable to the zeolitic crystallization [18–20]. In contrast, the hydrothermal synthesis of Ti-MWW is possible under alkali-free conditions [8]. Since the colloidal silica source contained impurity sodium, the effect of sodium on the crystallization of Ti-MWW was first investigated using alkali-free fumed silica of Cab-o-sil. The MWW phase was obtained from the

dry gels free of sodium using either HMI or PI as an SDA (Table 1, Nos. 10 and 11, and Fig. 1f). However, when the sodium content of the dry gel was increased by adding additional sodium hydroxide, the MWW phase was hardly formed at a Si/Na ratio of 5 and only amorphous phase was obtained at Si/Na ratios of 3 and 1 (Table 1, Nos. 12–14). Above results indicate that sodium is not essential for the formation of MWW phase in the DGC synthesis.

The DGC method exhibited a significant superiority over the hydrothermal synthesis method in reducing the amount of crystallization-supporting agent of boric acid, which made Ti-MWW crystallize at a Si/B ratio of 5 (Table 1). Nevertheless, there is still a large room for further decreasing the amount of boric acid because the Si/B ratio of both Ti-MWW-HTS and Ti-MWW-DGC is always around 11–17 in spite of far lower Si/B ratios in the gel.

We have made an attempt to synthesize Ti-MWW from the dry gels with higher Si/B ratios using the seeding technique. The seeding method has been verified to accelerate the growth of crystals in the case of hydrothermal synthesis of MCM-22 [21]. A deboronated MWW zeolite having a Si/B ratio of 46 was adopted as a seed. Table 2 lists the gel compositions and the compositions of products, while Figs. 3 and 4 show the typical XRD patterns for several as-synthesized products. The seed-containing dry gel showed the weak diffraction peaks due to remaining MWW structure (Table 2, Nos. 16–18 and Fig. 3a). Heating the B-free dry gel over HMI steam led to a product which showed basically the same XRD pattern (Fig. 3b), suggesting that the crystallization did not occur even with the support of seed. The XRD peak intensities due to the MWW phase increased with decreasing Si/B ratio and Ti-MWW samples with high crystallinity were obtained at a Si/B ratio of 12 (Fig. 3c–e). The SDA of PI also resulted in highly crystalline Ti-MWW at a Si/B ratio of 12 (Table 2, No. 19 and Fig. 3f). The crystallization completed at a Si/B of 5 within 1 week (Table 2, Nos. 20 and 21), while it took at least 2 weeks to obtain Ti-MWW without seed as described above.

With the support of seed, Ti-MWW was also easily crystallized from fumed silica. Although the product synthesized at a Si/B ratio of ∞ -12 still contained some amorphous phase (Fig. 4a and b, and Table 2, Nos. 22 and 23), Ti-MWW samples fully crystallized within 1 week at Si/B ratios of 8 and 5 using HMI or PI as an SDA (Fig. 4c–e and Table 2, Nos. 24–27). Furthermore, when 50 wt.% of seed relative to the silica was used, Ti-MWW lamellar precursor was also obtained even though the Si/B ratio of the gel was as high as 92 (the B species originated from the seed only), and the product contained much less B (Table 2, No. 28). Whether the formation of lamellar Ti-MWW precursor at such a high seed content was due to the ordinary crystallization or a sort of postsynthesis is still a subject of controversy. We can conclude from the above results that the seeding method effectively reduced the amount of boric acid in the synthesis of Ti-MWW and shortened the crystallization time as well.

Table 2
Synthesis results of Ti-MWW-DGC by seeding method^a

No.	Silica source	Gel composition			SDA	Time (week)	Product		
		Si/Ti	Si/B	Si/Na			Phase ^b	Si/Ti	Si/B
15	Colloidal + seed (10%)	60	∞	37	HMI	2	Amor.		
16	Colloidal + seed (10%)	60	20	37	HMI	3	Amor. + MWW		
17	Colloidal + seed (10%)	60	15	37	HMI	3	Amor. + MWW		
18	Colloidal + seed (10%)	60	12	37	HMI	2	MWW	63	18
19	Colloidal + seed (10%)	60	12	37	PI	2	MWW	63	18
20	Colloidal + seed (10%)	60	5	37	HMI	1	MWW		
21	Colloidal + seed (10%)	60	5	37	PI	1	MWW	84	14
22	Cab-o-sil + seed (10%)	60	∞	∞	HMI	2	Amor.		
23	Cab-o-sil + seed (10%)	60	12	∞	PI	3	Amor. + MWW		
24	Cab-o-sil + seed (10%)	60	8	∞	PI	1	MWW	58	14
25	Cab-o-sil + seed (10%)	60	5	∞	HMI	1	MWW		
26	Cab-o-sil + seed (10%)	60	5	∞	PI	1	MWW	86	14
27	Cab-o-sil + seed (10%)	30	5	∞	PI	1	MWW	28	13
28	Cab-o-sil + seed (50%)	30	92	∞	PI	1	MWW	49	155

^a Crystallization temperature 443 K.

^b Amor.: amorphous.

3.2. Physicochemical properties of Ti-MWW-DGC

Fig. 5 shows the scanning electron microscope (SEM) images of Ti-MWW-HTS and Ti-MWW-DGC samples. The large particles were considered the secondary crystals intergrown and aggregated from the primary thin platelet crystals of the MWW phase. The primary particle of Ti-MWW-HTS had an average size of ca. 0.4 μm , while that of Ti-MWW-DGC was approximately 10–20 times larger. The crystal size of Ti-MWW-HTS was found to depend on the SDA, PI favoring the formation of smaller crystals than HMI [8]. Taking into account the well known fact that the crystal size gives great influence to the catalytic performance through the diffusion limitation to the substrate molecules particularly in the liquid-phase, a lot of efforts have been made to prepare Ti-MWW-DGC with a small crystal size by varying the SDA, silica source, Si/B ratio, and Si/Na ratio, etc. as shown in Tables 1 and 2. Unfortunately, no Ti-MWW-DGC with a crystal size comparable to or smaller than

Ti-MWW-HTS was obtained. This result is also opposite to the phenomenon observed in the DGC synthesis of Ti-Beta, where the DGC synthesis generally leads to Ti-Beta with a much smaller crystal size than the hydrothermal synthesis [18–20]. Thus, there is an essential difference in the mechanism of zeolite crystallization between Ti-MWW-DGC and Ti-Beta-DGC. The large crystal size of Ti-MWW-DGC is probably due to a smaller number of nuclei formed at initial crystallization stage.

The UV–vis spectra of as-synthesized Ti-MWW-DGC showed two bands around 220 and 260 nm regardless of various synthesis conditions (Fig. 6). The 220 nm band is attributed to the charge transfer from O^{2-} to tetrahedrally coordinated Ti^{4+} which is highly dispersed in the zeolite framework, and is characteristic of Ti-substituted molecular sieves [1,2]. The 260 nm band is generally assigned to the octahedral nonframework Ti species. The occurrence of octahedral Ti species should not be the peculiar case of the DGC method since previous hydrothermal synthesis also

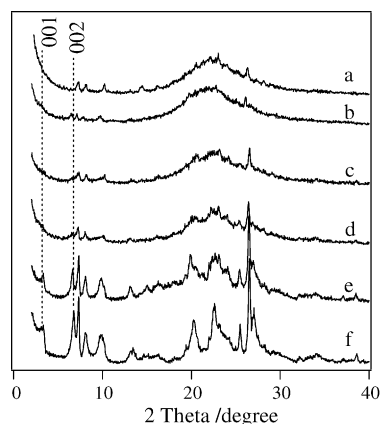


Fig. 3. XRD patterns of seed-containing dry gel (a) and as-synthesized Ti-MWW-DGC prepared with seeding method from colloidal silica and HMI at Si/B ratio of ∞ (b), 20 (c), 15 (d), and 12 (e), and from PI at Si/B ratio of 12 (f).

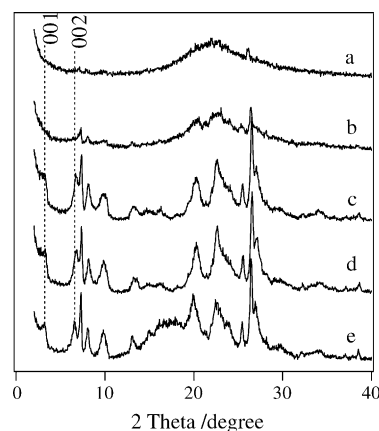


Fig. 4. XRD patterns of as-synthesized Ti-MWW-DGC prepared with seeding method from fumed silica at Si/Ti ratio of 60 and Si/B ratio of ∞ (a), 12 (b), 8 (c), and 5 (d), at Si/Ti ratio of 30 and Si/B ratio of 5 (e).

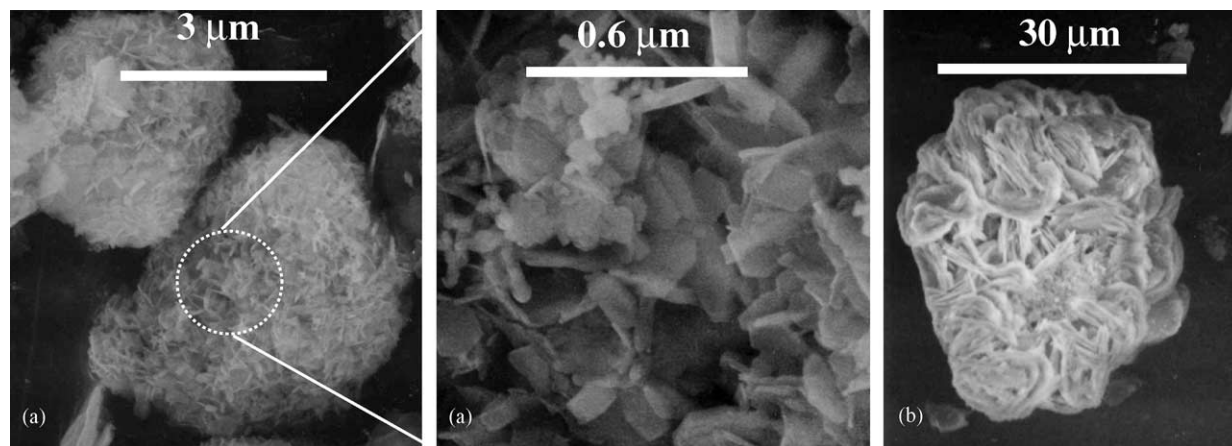


Fig. 5. SEM images of Ti-MWW-HTS (a) and Ti-MWW-DGC (b).

resulted in the incorporation of nonframework Ti [8]. This has been presumably related to the lamellar structure of the MWW precursor. The precursor contains a large amount of layer sheets on the surface of which Ti would tend to form the octahedral species. Despite of the presence of the octahedral species with the 260 nm band, the absence of 330 nm band indicated that nearly no anatase-like Ti phase was formed on the Ti-MWW-DGC samples. It should be noted that very weak bands were observed in the region over 300 nm especially in Fig. 6d and e. Generally, DGC-prepared samples was of brown color as a result of the decomposition of amine template. The colored organic species then presumably correspond to those bands.

Acid treatment has been carried out with the purpose of removing the catalytically non-active octahedral Ti species. When as-synthesized Ti-MWW-DGC samples were refluxed

in 2 M HNO₃ solution and subsequently calcined at 873 K, the nonframework species were removed selectively, while only tetrahedral Ti species remained in the MWW structure, which was evidenced by the sole UV–vis band at 220 nm (Fig. 7). Compared with acid-treated Ti-MWW-HTS (Table 3, Nos. 29 and 30), acid-treated Ti-MWW-DGC had similar Si/B ratios in the case of non-seeding method (Table 3, Nos. 32–35) while higher Si/B ratios for seeding method (Table 3, Nos. 36–39). However, the acid treatment removed much more Ti to result in Ti-MWW-DGC with high Si/Ti ratios, suggesting that a large part of Ti species incorporated by the DGC method are in the nonframework sites and therefore less stable upon the acid treatment.

The acid treatment and calcination led to the samples with three dimensional MWW structure and high crystallinity (Fig. 8). Moreover, the nitrogen adsorption measurements revealed that all the acid-treated and further calcined

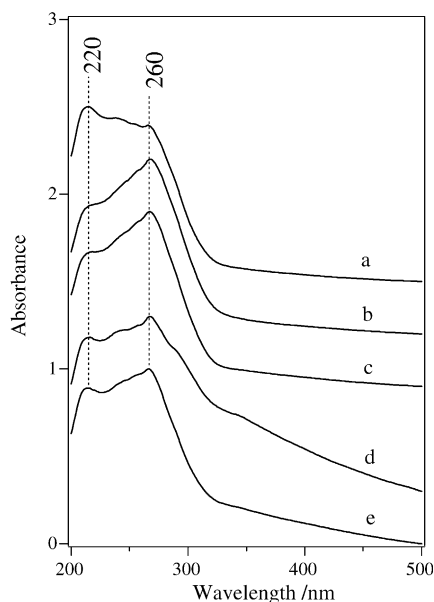


Fig. 6. UV–vis spectra of as-synthesized Ti-MWW-DGC samples corresponding to those in Table 2, No. 18 (a), No. 24 (b), No. 25 (c), No. 26 (d) and No. 28 (e).

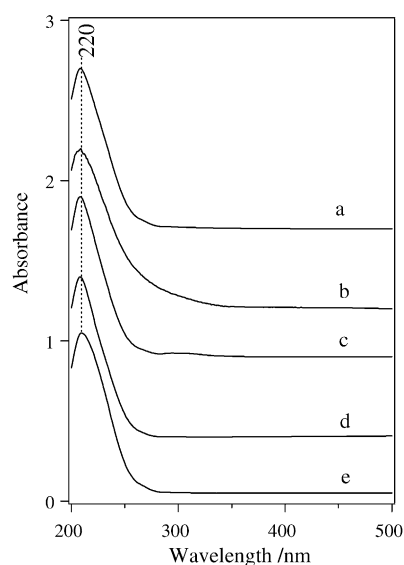


Fig. 7. UV–vis spectra of Ti-MWW-DGC samples after acid-treatment and calcination at 873 K. The samples were prepared from the as-synthesized ones in Fig. 6.

Table 3
Chemical composition of Ti-MWW and the results of epoxidation of hex-1-ene with H₂O₂^a

No.	Preparation method	Silica source	SDA	Chemical composition					SA ^b (m ² /g ⁻¹)	Epoxidation of hex-1-ene			
				As-synthesized			Acid-treated ^c			Hex-1-ene conversion (mol%)	TON (mol(mol Ti) ⁻¹)	H ₂ O ₂ (mol%)	
				Si/Ti	Si/B	Si/Na	Si/Ti	Si/B				Conversion	Selectivity
29	HTS, No.1	Cab-o-sil	PI	51	11	∞	72	39	624	23.5	222	26	92
30	HTS	Cab-o-sil	PI	31	11	∞	47	36	615	32.8	189	35	94
31 ^d	HTS	Cab-o-sil	PI				59	559	624	26.8	193	37	72
32	DGC, No.5	Colloidal	HMI	61	17	114	315	31		0.7	27	0.8	91
33	DGC	Colloidal	HMI	71	17	100	328	40		0.9	34	11	8
34	DGC, No.9	Colloidal	PI	84	14		244	52	566	4.0	120	9	44
35	DGC, No.10	Cab-o-sil	HMI	84	14	∞	223	63	528	2.8	78	19	16
36	DGC-seeding 10%, No.18	Colloidal	HMI	63	18	73	265	35		0.9	28	1.2	72
37	DGC-seeding 10%, No.21	Colloidal	PI	84	14	454	238	184		2.4	69	7	33
38	DGC-seeding 10%, No.24	Cab-o-sil	PI	58	14	∞	215	153		1.7	42	7	26
39	DGC-seeding 10%	Cab-o-sil	PI	56	12	∞	191	200		4.2	96	8	49
40	DGC-seeding 50%	Cab-o-sil	PI	48	141	∞	150	–	–	26.7	482	29	92

^a Epoxidation conditions: hex-1-ene, 10 mmol; H₂O₂ (31 wt.%), 10 mmol; MeCN, 10 mL; temperature, 333 K; time, 2 h.

^b SA = surface area (Langmuir).

^c Refluxed with 2 M HNO₃.

^d Obtained by treating No. 30 sample with 2 M HNO₃.

samples had Langmuir specific surface areas over 500 m² g⁻¹. It is concluded from the above results that Ti-MWW containing isomorphously substituted Ti in the framework was successfully prepared by a combination of the DGC method and post-acid treatment.

3.3. Catalytic properties of Ti-MWW-DGC

The catalytic properties of Ti-MWW-DGC have been investigated in the epoxidation of hex-1-ene with H₂O₂ in comparison with those of Ti-MWW-HTS. Ti-MWW-HTS catalysts with different Ti contents showed comparable

specific activity, i.e. turnover number (TON) for hex-1-ene conversion and high efficiency of H₂O₂ utilization (Table 3, Nos. 29 and 30). When the B species were thoroughly removed by further acid treatment, the TON remained nearly the same (Table 3, No. 31), suggesting the coexistent B affected negligibly the catalytic behavior of framework Ti at least when Si/B ratio was over 30.

The Ti-MWW-DGC catalysts showed much lower conversion for hex-1-ene than the Ti-MWW-HTS samples reasonably due to their much lower Ti contents (Table 3, Nos. 32–39). Not only the apparent activity, the intrinsic activity per Ti site, TON also fell greatly behind Ti-MWW-HTS. The efficiency of H₂O₂ utilization was much lower as a result of nonproductive decomposition. The TON of Ti-MWW-DGC increased slightly although conscious efforts have been made in changing various synthesis factors. The lower TON was hardly attributed to the crystallinity, the surface area, the Ti states or the B content because Ti-MWW-DGC was found to be similar in the properties to Ti-MWW-HTS. Thus, the crystal size is assumed to be the plausible reason for the difference in TON between two kinds of Ti-MWW catalysts. The diffusivity of molecules is inversely proportional to the square of the average size of adsorbent particles [22]. Ti-MWW-DGC which was 10–20 times larger than Ti-MWW-HTS in crystal size as shown above, should imposed serious diffusion problem for the substrate molecules accessing to the Ti sites and also for the product molecules diffusing out of the zeolite channels. The bulky Ti-peroxo intermediate species formed by the interaction of H₂O₂ with Ti species would further enhance

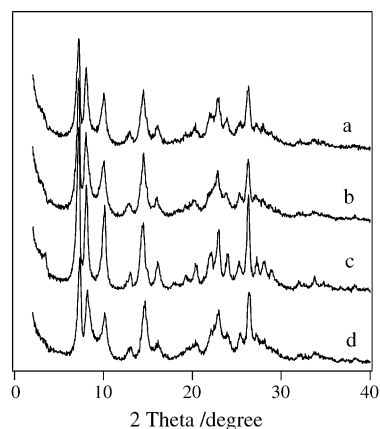


Fig. 8. XRD patterns of Ti-MWW-DGC samples after acid-treatment and calcination. The samples corresponded to those in Table 2, No. 24 (a), No. 25 (b), No. 26 (c) and No. 28 (d).

the diffusion problem imposed by larger crystal titanosilicate catalysts [23]. Nevertheless, Ti-MWW-DGC prepared by using 50% seed proved to be a very active catalyst which showed a TON even larger than Ti-MWW-HTS (Table 3, No. 40). Although it is still a matter under consideration whether a real crystallization has taken place or the Ti has been post-incorporated into the framework of deboronated MWW, the DGC shows a potential for Ti-MWW catalysts.

4. Conclusions

Ti-MWW has been synthesized for the first time by the DGC method from the colloidal and fumed silica sources with the assistance of boric acid by using the SDAs of piperidine and hexametheleneimine. The crystallization of Ti-MWW takes place under either alkali-free or alkali-containing conditions, but too high content of sodium in the dry gel suppresses the crystallization. The amount structure-supporting agent of boron can be greatly reduced in the DGC method and further by adding the seed. Although the DGC method leads to the incorporation of both the tetrahedral and octahedral Ti species into the MWW precursors, the latter are selectively removed by acid treatment. DGC-synthesized Ti-MWW is less active in the epoxidation of hex-1-ene with H_2O_2 than hydrothermally synthesized one because of much larger crystal size.

Acknowledgements

MH thanks the financial supports by National Natural Science Foundation of China (Grant No. 20233030) and Science and Technology Commission of Shanghai Municipality (03DJ14005).

References

- [1] B. Notari, *Adv. Catal.* 41 (1996) 253.
- [2] G. Bellussi, M.S. Rigutto, *Stud. Surf. Sci. Catal.* 137 (2001) 911.
- [3] M. Taramasso, G. Perego, B. Notari, US Patent 4 410 501 (1983).
- [4] J.S. Reddy, R. Kumar, P. Ratnasamy, *Appl. Catal.* 58 (1990) 1.
- [5] (a) M.A. Cambor, A. Corma, A. Martínez, J. Pérez-Pariente, *J. Chem. Soc., Chem. Commun.* (1992) 589;
(b) J.C. van der Waal, P.J. Kooyman, J.C. Jansen, H. van Bekkum, *Micropor. Mesopor. Mater.* 25 (1998) 43.
- [6] P. Wu, T. Komatsu, T. Yashima, *J. Phys. Chem.* 100 (1996) 10316.
- [7] M. Diaz-Cabanas, L.A. Villaescusa, M.A. Cambor, *Chem. Commun.* (2000) 761.
- [8] P. Wu, T. Tatsumi, T. Komatsu, T. Yashima, *J. Phys. Chem. B* 105 (2001) 2897.
- [9] P. Wu, T. Tatsumi, T. Komatsu, T. Yashima, *J. Catal.* 202 (2001) 245.
- [10] P. Wu, T. Tatsumi, *Chem. Commun.* (2001) 897.
- [11] P. Wu, T. Tatsumi, *J. Phys. Chem. B* 106 (2002) 748.
- [12] P. Wu, T. Tatsumi, *Chem. Commun.* (2002) 1026.
- [13] W. Xu, J. Dong, J. Li, F. Wu, *J. Chem. Soc., Chem. Commun.* (1990) 755.
- [14] P.R.H.R. Rao, M. Matsulata, *Chem. Commun.* (1996) 1441.
- [15] M. Matsukata, N. Nishiyama, K. Ueyama, *Micropor. Mater.* 7 (1996) 109.
- [16] N. Nishiyama, K. Ueyama, M. Matsukata, *Micropor. Mater.* 7 (1996) 299.
- [17] R. Bandyopadhyay, Y. Kubota, N. Sugimoto, Y. Fukushima, Y. Sugi, *Micropor. Mesopor. Mater.* 32 (1999) 81.
- [18] N. Jappar, Q.H. Xia, T. Tatsumi, *J. Catal.* 180 (1998) 132.
- [19] T. Tatsumi, N. Jappar, *J. Phys. Chem. B* 102 (1998) 7126.
- [20] M. Ogura, S. Nakata, E. Kikuchi, M. Matsukata, *J. Catal.* 199 (2001) 41.
- [21] I. Mochida, S. Eguchi, M. Hironaka, S. Nagao, K. Sakanishi, D.D. Whitehurst, *Zeolites* 142 (18) (1997).
- [22] J. Karger, D.M. Ruthven, *Diffusion in Zeolite*, Wiley, New York, 1992, p. 230.
- [23] P. Wu, T. Komatsu, T. Yashima, *J. Phys. Chem. B* 102 (1998) 9297.